WDM DEVICE FOR OPERATION IN THE VISIBLE SPECTRUM

Tiago Silva, Paula Louro, Manuela Vieira
ADEETC, Instituto Superior de Engenharia de Lisboa (ISEL), Lisbon, Portugal
30295@alunos.isel.pt

Keywords: Optoelectronics, Wavelength Division Multiplexing.

Abstract: This paper presents results on the use of multilayered a-SiC:H heterostructures as a device for wavelength-division demultiplexing of optical signals in the visible range. A demux algorithm was implemented to extract the information carried on by each input optical channel. The algorithm makes use of the device wavelength dependence on applied electric bias and optical background bias.

1. INTRODUCTION

WDM is a standard technique used to enlarge the bandwidth of a transmission channel through the simultaneous transmission of different signals encoded in the same path. In optical communication systems in the infrared window the devices used perform the mux and demux operations usually employ optical filters based on prisms, interference filters, diffraction gratings or arrayed waveguide grating (AWG). For the visible range the shift on the wavelength demands the conversion of such devices or alternatively the use of novel approaches to perform the same operation. Optical communications in the visible range have important applications the field dominated by short range communications, such as, home networks, automotive industry of traffic control applications as well as industrial purposes.

In this paper we report the use of a device based on p-i'(a-SiC:H)-n/p-i(a-Si:H)-n heterostructure optimized for the detection of the short and long wavelengths in the visible range. The thickness and the absorption coefficient of the i'- and i- layers were tailored for short and long waelengths optical confinement, respectively in the front and back photodiodes acting both as optical filters. Its sensitivity can be tuned either by the external electrical bias or the optical bias.

The recovery of the input optical channels is done through the use of the multiplexed signal sampled at reverse and forward bias, or by the signal acquired with and without optical bias. A demux algorithm was developed using Excel/Visual Basic to recover from the combined output signal the information transmitted by each optical channel.

2. DEVICE CONFIGURATION

The device described herein operates from 400 to 700 nm which makes it suitable for operation at visible wavelengths in optical communication applications. The device is a multilayered heterostructure based on a-Si:H and a-SiC:H. The configuration of the device includes two stacked p-i-n structures between two electrical and transparent contacts (Fig. 1). Both front and back structures act as optical filters confining, respectively, the short and the long optical carriers, while the intermediate wavelengths are absorbed across both [i,ii]. The device was operated within the visible range using as optical signals, to simulate the transmission optical channel, the modulated light (external regulation of frequency and intensity) supplied by a red, a green and a blue LED with wavelengths of 470 nm, 524 nm and 626 nm, respectively. (Fig. 1).

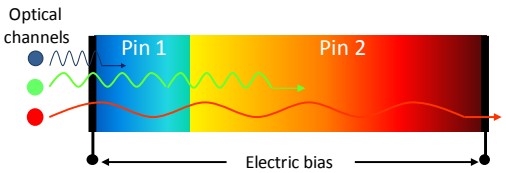

Figure 1 WDM device configuration.

3. OPTOELECTRONIC CHARACTERISATION

3.1 Effect of the electrical voltage

The device spectral sensitivity in the visible range measured under reverse and forward bias is displayed in Fig. 2

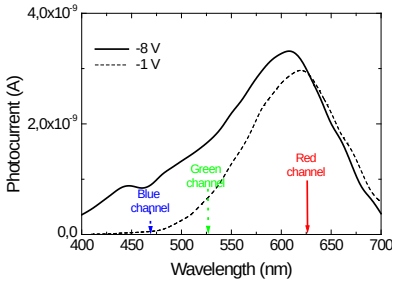

Figure 2 Spectral photocurrent at reverse and forward bias.

The experimental results (Fig. 2) show that under red wavelength modulated light the photocurrent signal, obtained under reverse and forward bias is similar, which suggests a weak dependence on the applied voltage. For shorter wavelengths the behavior is quite different, as the signal exhibits a strong decrease under forward bias. For the blue wavelength the signal is suppressed.

3.2 Effect of the optical bias

The transient photocurrent signal obtained through the optical excitation of each transmission channel was measured at reverse bias using additional steady state illumination as background optical bias. Results for each channel are displayed in Fig. 3.

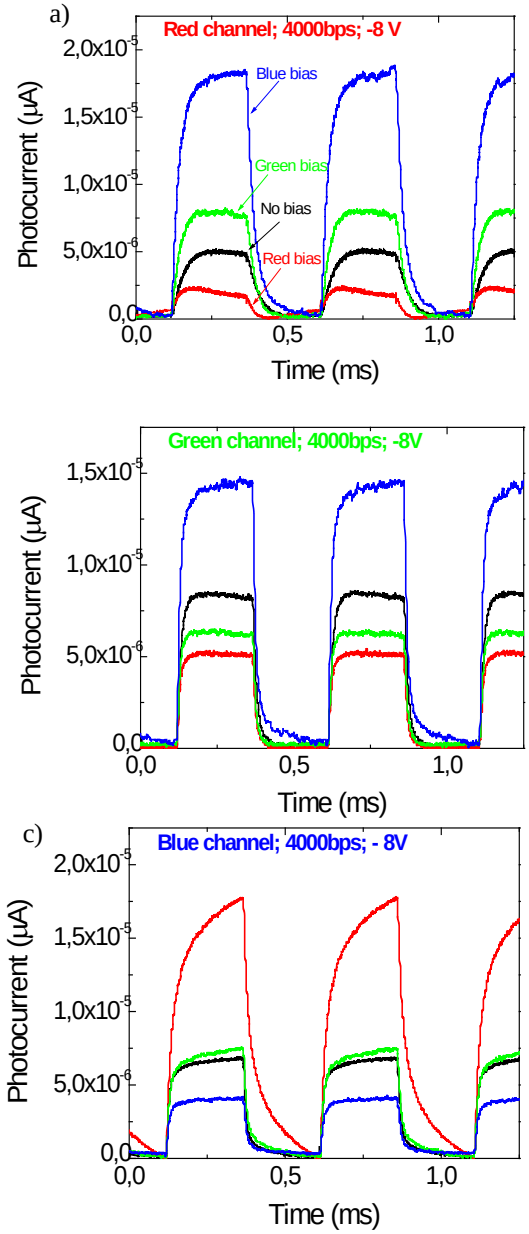

Figure 3 (a) red (b) green and (c) blue channels under reverse and forward voltages without and with red, green and blue optical bias.

3.3 Multiplexed signal

In Figure 4 it is shown the multiplexed signals, under reverse and forward bias, obtained with one RGB bit sequences.

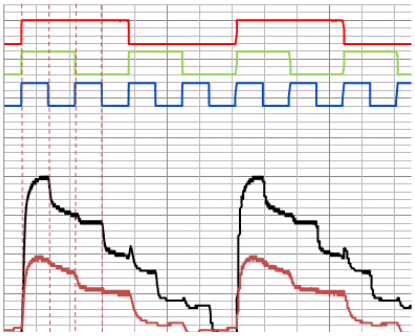

Figure 4 - Multiplexed signals, under reverse and forward bias, obtained with one RGB bit sequence.

It is observed that the photocurrent, under the multiple combinations of optical signals and reverse bias, exhibits eight different levels that correspond each to different optical bias states. Under forward bias the signal magnitude decreases as suggested by the results of the photocurrent-wavelength characteristics (Fig. 2).

The extinction of the blue photocurrent signal component under forward bias allows the identification of the three input channels (color and transmission speed) by comparing the different threshold magnitudes of the multiplexed signals under forward and reverse bias. The variation of the signal under reverse and forward bias is the basis for the recognition of each input channel.

4. RECOVERY OF THE INPUT CHANNELS

The recovery of the input channels was done taking advantage of the device spectral sensitivity dependence on the electrical and optical bias.

The algorithm used for the automatic recognition of the optical signals transmitted by each channel was developed under Excel/Visual Basic. This task was divided into 5 sub-tasks, namely, “Data normalization”, “Evaluation of bit duration”, “Bit start”, “Selection of the 8 bits”, “Evaluation of Mode”.

4.1 Data Normalization

The output signal was split into two components: time and magnitude. In the magnitude domain the minimum value of magnitude was added and then divided by the difference between the maximum and the minimum. The signal was reconstructed joining the normalized magnitude with the time domain.

4.2 Evaluation of the bit duration

In this task the purpose is the identification the transmitted sequence extent and the evaluation of the amount of samples necessary to identify 1 Bit. The time of a bit, for a sequence transmitted at 6000 bps is given by:

$$Tempo\ Bit = \frac{1bit}{Bit\ Rate} = \frac{1}{6000} = 167\ ms$$

The number of samples necessary for the description of the bit is evaluated by:

$$Amostras/Bit = \frac{nº\ amostras \times tempo\ Bit}{tempo\ maximo\ das\ amostras} =$$

$$\frac{2500 \times 0{,}000167}{0{,}0025} = 166{,}666$$

This means that it is necessary to use 167 samples for the complete description of each bit, and 1336 samples for the whole sequence (8 bits).

4.3 Bit start

The determination of the bit start is one of the basic steps to implement the algorithm, as it depends on the acquisition conditions (Figure 4).

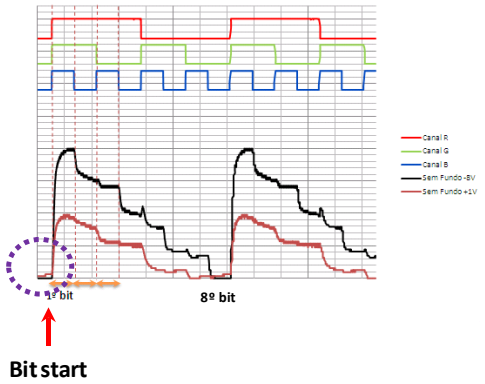

Figure 4 Example of a photocurrent signal measured at – 8V for a 8 bit sequence transmitted at 6000 bps.

The bit start of the signal, made of 2500 samples, was obtained through the first derivative of the measured signal, which was evaluated using the expression:

$$Diff\,(i) = [\,i(10) - i(1);\, i(11) - i(2);\ldots;\, i(2500) - i(2490)]$$

In figure 5 it is displayed the first derivative of the signal.

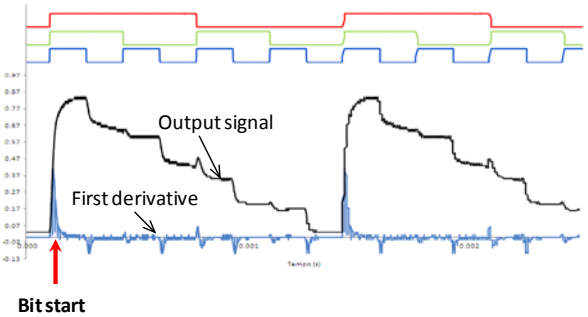

Figure 5 - Photocurrent signal and its first derivative.

Results from Fig. 5 show that the sharp transitions of the first derivative correspond to changes of the photocurrent signal threshold, i. e., to changes of the photocurrent magnitude caused by different optical conditions.

4.4 Selection of the 8 bit sequence

At this stage it is necessary to select sample of 8 bits that constitute the transmitted sequence. This is done using for the first sample the Start bit and adding then the following 1366 samples to describe the 8 bits, as can be seen in Figure 6.

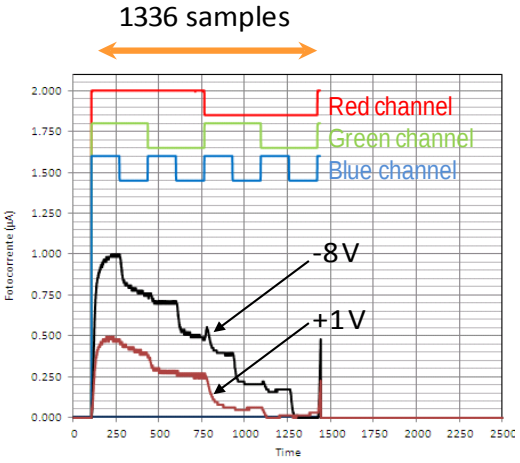

Figure 6 Identification of a complete sequence of 1336 samples in the acquired signal.

4.5 Evaluation of the mode

In this step it is necessary to identity the photocurrent thresholds associated to each optical excitation state.

This was implemented using the statistical indicator mode over a representative range of samples contained in the167 samples of each bit (figure 7).

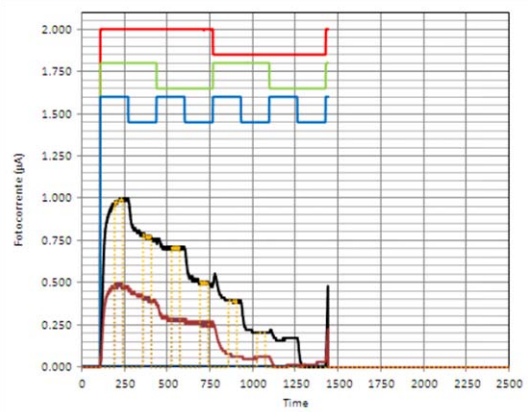

Figure 7 – Graphical representation of the standard sequence

Bits	Steps		OUTPUT s/bck			
			RGB -8V	RGB +1V		
			MODA	MODA	INPUT	RGB
1°	189	239	0.984	0.476		
2°	356	406	0.778	0.397		
3°	523	573	0.698	0.286		
4°	690	740	0.492	0.254		
5°	857	907	0.397	0.063		
6°	1024	1074	0.206	0.063		
7°	1191	1241	0.175	0.016		
8°	1358	1408	0.000	0.032		
					INPUT s/bck	

In Table I it is displayed as an example the mode values correspondent to the ranges selected in the thresholds of Fig. 7.

Table I - Table to the ranges selected in the thresholds of Fig. 7

5. RESULTS AND DISCUSSION

In this section we present example of the output demux algorithm obtained for input different sequences. The algorithm was used either using the voltage variation and the optical bias dependence.

5.1 Effect of the electrical voltage

From the analysis of the data obtained measuring the output signal using different input sequences under reverse and forward bias it was concluded that some optical states originate similar threshold values. In order to overcome this problem the similar threshold photocurrents were joined together in order to decrease the number of available states, which at -8 V corresponds to the five combinations: RGB; RG+RB; R+GB; G+B; OFF. At forward bias only 4 states are available due to the suppression of the blue component (RG; R; G; OFF).

The results of the data analysis of the output signal measured using different input sequences it shown in Table II.

S/ Background					
s/bck	RGB	RG+RB	R+GB	G+B	OFF
-8V	[1.00 0.94]	[0.915 0.69]	[0.61 0.25]	[0.24 0.023]	[0.02 0]
s/bck	RG	R	G	OFF	
+1V	[0.55 0.38]	[0.38 0.20]	[0.19 0.05]	[0.04 0.00]	

Table II – Table with the ranges for each possible sequence of bits.

In Figure 8 it is displayed an example of the automatic recognition of the input sequence R[10110010], G[00101110], B[11001010], transmitted at 6000 bps.

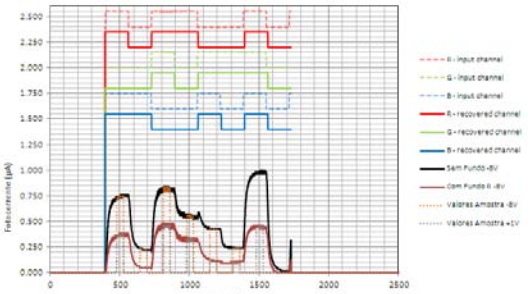

Figure 8 – Graphical representation of the sequence above.

Bits	Steps		OUTPUT s/bck			
			RGB -8V	RGB +1V		
			MODA	MODA	INPUT	RGB
1°	476	526	0.746	0.365	RB	101
2°	643	693	0.222	0.048	B	001
3°	810	860	0.810	0.444	RG	110
4°	977	1027	0.540	0.333	R	100
5°	1144	1194	0.429	0.127	GB	011
6°	1311	1361	0.238	0.111	G	010
7°	1478	1528	0.968	0.444	RGB	111
8°	1645	1695	0.016	0.000	OFF	000
					INPUT s/bck	

In Table III it is displayed the data related to the individual recognition of each input channel.

As can be seen in figure 8 the match between the input sequence of each channel and automatic recognition is complete. The algorithm was tested, under the same experimental conditions, for a wide range of bit sequences.

5.2 Effect of the optical bias

The use of the optical bias for the channel recognition will use the similar suppression of the channel when using optical bias of the same wavelength. This principle was the basis for the algorithm implementation, using the signal measured under reverse bias, without and with optical bias.

In Figure 9 it is displayed the output signals measured at -8 V without optical bias and with red optical bias.

In the top of the figure there are displayed the input sequences of each channel and the sequence recognized by the application of the algorithm, that exhibits a correct match.

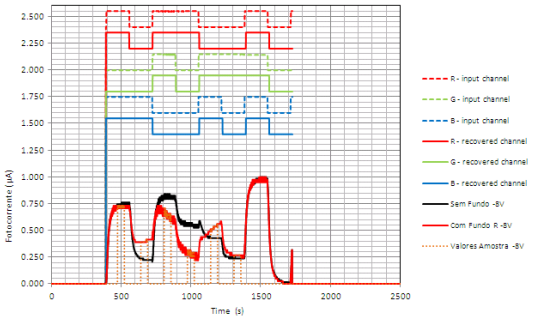

Figure 9 – Graphical representation of the output sequence R[10110010], G[00101110], B[11001010] without optical bias and with red optical bias.

In Table IV it is displayed the data analysis related to the signals measured with and without optical bias, and in Table V it is displayed the data related to the individual recognition of each input channel.

C/ RED Background								
-8V	RGB	RG	RB	R	GB	G	B	OFF
S/bck - R	>	>	>	>	<	>	<	>
C/bck	0.052	0.400	0.200	0.422	-0.430	0.170	-0.350	0.030
%	-5%	-40%	-20%	-42%	43%	-17%	35%	-3%

Table IV - Table with the ranges for each possible sequence of bits with red background application.

Bits	Steps		OUTPUT s/bck				OUTPUT bck R		
			RGB -8V	RGB +1V			RGB -8V		
			MODA	MODA	INPUT	RGB	MODA	INPUT	RGB
1°	476	526	0.746	0.365	RB	101	0.732	RB	101
2°	643	693	0.222	0.048	B	001	0.390	B	001
3°	810	860	0.810	0.444	RG	110	0.659	RG	110
4°	977	1027	0.540	0.333	R	100	0.293	R	100
5°	1144	1194	0.429	0.127	GB	011	0.537	GB	011
6°	1311	1361	0.238	0.111	G	010	0.268	G	010
7°	1478	1528	0.968	0.444	RGB	111	0.951	RGB	111
8°	1645	1695	0.016	0.000	OFF	000	0.000	OFF	000
					INPUT s/bck			INPUT bck R	

Table V - it is displayed the data related to the individual recognition of each input channel with red background application.

As can be seen the statistical data of Tables IV and V relate to the characterisation of each photocurrent threshold with and without red optical bias. The variations associated to the presence of the red background light induce a strong reduction of the red channel and an increase of the blue channel. This effect results in the establishment of new photocurrent levels that give information to decode the input signals.

6. CONCLUSION

A multilayered device based on a-SiC:H/a-Si:H was used for demultiplexing optical signals operating in the visible range. The effect of the electrical applied voltage and of the use of steady illumination was analyzed. A recovery algorithm to demultiplex the optical signals was proposed and tested.

Future work related to the automatic recognition of the input signals, include the optimization for operation at different optical powers and transmission frequencies.

REFERENCES

Michael Bas, Fiber Optics Handbook, Fiber, Devices and Systems for Optical
Communication, Chap, 13, Mc Graw-Hill, Inc. 2002.

M.Bas, Fiber Optics Handbook, Fiber, Dev.and Syst. for Opt. Comm., Chap, 13, Mc Graw-Hill, 2002.

M. Vieira, M. Fernandes, P. Louro, A. Fantoni, Y. Vygranenko, G. Lavareda, C. Nunes de Carvalho, Mat. Res. Soc. Symp. Proc., Vol. 862 (2005) A13.4.

P. Louro, M. Vieira, M.A. Vieira, M. Fernandes, A. Fantoni, C. Francisco, M. Barata, Physica E: Low-dimensional Systems and Nanostructures, 41 (2009) 1082-1085.

M. A. Vieira, M. Vieira, J. Costa, P. Louro, M. Fernandes, A. Fantoni, in Sensors & Transducers Journal Vol. 9, Special Issue, 2010, pp.96-120..